Comprehensive study of noise processes in electrode electrolyte interfaces

Arjang Hassibi,[a] Reza Navid, Robert W. Dutton, and Thomas H. Lee
Center for Integrated Systems, Department of Electrical Engineering, Stanford University, Stanford, California 94305-4070

(Received 16 January 2004; accepted 4 April 2004)

A general circuit model is derived for the electrical noise of electrode–electrolyte systems, with emphasis on its implications for electrochemical sensors. The noise power spectral densities associated with all noise sources introduced in the model are also analytically calculated. Current and voltage fluctuations in typical electrode–electrolyte systems are demonstrated to originate from either thermal equilibrium noise created by conductors, or nonequilibrium excess noise caused by charge transfer processes produced by electrochemical interactions. The power spectral density of the thermal equilibrium noise is predicted using the fluctuation-dissipation theorem of thermodynamics, while the excess noise is assessed in view of charge transfer kinetics, along with mass transfer processes in the electrode proximity. The presented noise model not only explains previously reported noise spectral densities such as thermal noise in sensing electrodes, shot noise in electrochemical batteries, and $1/f$ noise in corrosive interfaces, it also provides design-oriented insight into the fabrication of low-noise micro- and nanoelectrochemical sensors. [DOI: 10.1063/1.1755429]

I. INTRODUCTION

Electrode–electrolyte interfaces are an important part of most electrochemical systems, such as those used as energy sources, transducers, and sensors.[1,2] The measurable transport of charge across the electrode–electrolyte interface (i.e., electrical current) as well as the interface potential consists of a deterministic wave form and a randomly varying fluctuation, which substantiates the presence of noise processes. The noise of the electrode interface and the unpredictable relationship between the potential and the flowing current typically brings about a level of uncertainty in the system. Depending on the electrochemical system, this randomness may well result in an inaccurate measurement or an imprecise actuation. For instance, in work-function-based sensors [e.g., ion-sensitive field-effect transistor (ISFET)[3,4]], the noise of the electrode system, in addition to the noise of the FET, limits the accuracy of the analysis. Next to sensors, battery-operated systems also employ various ''noisy'' electrode-based energy sources.[5,6] Consequently, it is quite sensible to anticipate some negative effects from battery current fluctuations, on the performance and reliability of any battery-driven electronics. With the current trend towards the implementation of small-scale microfabricated electrochemical sensors,[7–11] a comprehensive understanding of microelectrode systems and their fidelity has become more essential. While in most electrochemical systems electrode noise elimination is impractical (e.g., shot noise of batteries), a comprehensive study of noise provides valuable insight for low-noise electrode and electrochemical system design. This result would, in fact, help designers make better-informed decisions about next generation microfabricated electrochemical sensors, as well as battery-operated systems.

Early studies of noise in electrode systems were formally presented by Tyagai[12] and Euler[13] and later by Blanc and co-workers[14–16] on electrochemical batteries and various faradaic electrodes. Their reports all indicated the presence of shot noise in batteries and galvanic processes in general. However, the exact magnitude of the reported noise varied between systems, usually as a function of the molecules participating in the redox reaction, as well as the electrical settings (i.e., load resistance and internal impedance of the cell). Yet, the area in which electrode noise became most attractive was corrosion monitoring. Iverson[17] was the first to apply noise measurement techniques to examine the corrosion of metals. The later work of Hladky and Dawson reintroduced this technique in 1981[18] and 1982,[19] in which they proposed that both qualitative and quantitative information about the corrosion attack can be obtained from the noise spectrum and its rms value. In their work, they also reported the presence of $1/f$ noise in slow corroding interfaces. This specific phenomenon occurs less frequently in galvanic systems with a high charge transfer rate.

While widespread research has been carried out on the characteristics of electrochemical noise in general,[20,21] less work has been reported on electrode noise modeling, and on the fundamental processes which create diverse spectra (i.e., $1/f$ noise versus Lorentzian noise). In this article, we establish a comprehensive model for electrode noise in its general form, which includes both faradaic and nonfaradaic electrodes. Initially in Sec. II, we will review the circuit model of electrode–electrolyte interfaces. Subsequently, in Sec. III, we will demonstrate that electrode noise can be categorized into thermal equilibrium noise created by conductors; nonequilibrium excess noise caused by charge transfer kinetics; and relaxation currents produced by mass transfer processes. As practical implications, these results are also employed to derive noise circuit models for ISFET sensors (a sensory

[a]Electronic mail: arjang@stanford.edu

system comprising of a nonfaradaic interface), and galvanic batteries (a faradaic system) in Sec. IV. It is also shown recurrently in the text that the predicted noise power spectral density matches the actual data previously reported in the literature.

II. ELECTRODE SYSTEMS

Generally speaking, two types of processes can occur at electrode–electrolyte interfaces. One kind comprises reactions in which charged particles such as electrons cannot pass across the interface barrier. In these interfaces, generally called nonfaradaic, no charge transfer reaction takes place since such processes (i.e., oxidation or reduction) are, in fact, thermodynamically unfavorable. The electrode in the nonfaradaic case is typically called an ideal polarized electrode (IPE), which behaves like an ideal capacitor. Although the interface is inert, processes such as absorption and desorption within the electrolyte might still occur as a result of varying potential or solution composition. It is imperative to understand that even if charge does not cross the IPE interface, external transient fluxes might still flow and be coupled to the electrode via interface capacitance, subsequent to sudden changes in potential, electrode area, or solution composition. Our treatment of these systems, however, only covers their thermal equilibrium state. The second type of electrode system is called faradaic. Under specific circumstances, any electrode–electrolyte interface will show a range of potentials in which charged particles such as electrons are able to pass across the interface. In faradaic electrodes, charge transfer typically imposes oxidation or reduction, which indicates that the charged species in dissimilar phases (typically electrons in the conductor and ions in the electrolyte) interact and pass on the net charge to one another.

For both faradaic and nonfaradaic electrodes, finding the electrical circuit model requires the understanding of ionic fluxes as well as their concentration profile. For systems in a nonequilibrium state such as faradaic electrodes, spatial fluxes are nonzero for at least one ionic species, in contrast with IPE systems in equilibrium where no net current exists. The concentration of ions and their fluxes, in general, specify the electrical model of the system. If we assume an electrolyte with m different ionic species ($m \geqslant 2$), the current flux of the ith charged species $\mathbf{J}_i$, with spatial concentration of n_i, is governed by the Nernst–Planck equation for mass transfer[1]

$$\mathbf{J}_i = -D_i \nabla n_i - \frac{z_i q}{kT} D_i n_i \nabla \Phi + n_i \boldsymbol{\nu}, \tag{1}$$

where D_i is the diffusion coefficient, Φ the spatial electrical potential, q the charge on an electron, k the Boltzmann constant, T the absolute temperature, $\boldsymbol{\nu}$ the convection vector, and z_i the (signed) average charge on ionic species i. The three terms on the right-hand side of Eq. (1) represent the contributions of diffusion, drift, and convection, respectively, to the flux. For the ith species, we can write the continuity equation that expresses the species concentration change as a function of time, such that

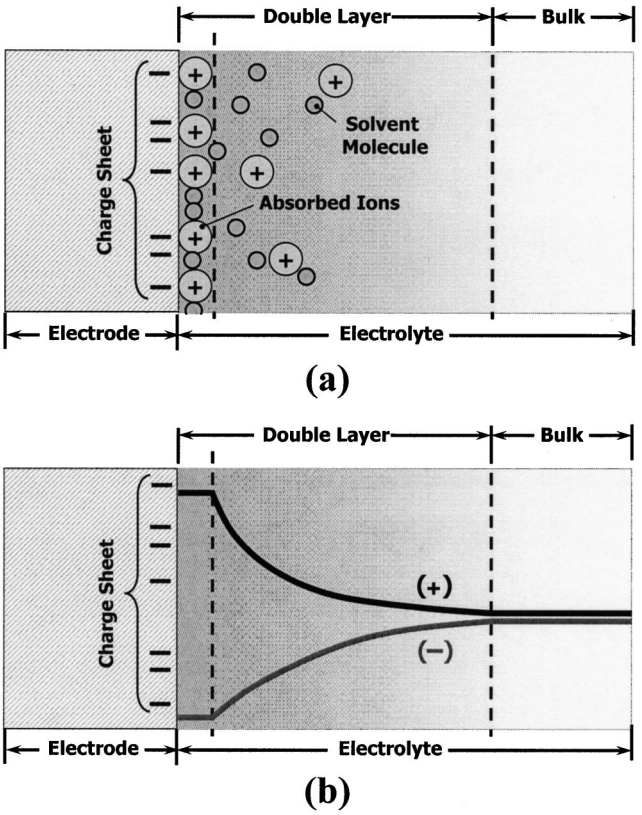

FIG. 1. Basic molecular-level structure of a nonfaradaic electrode (a), and (b) macroscopic charge distribution of the electrode in the diffusion and double layer.

$$\frac{\partial n_i}{\partial t} = G_i - R_i - \nabla \cdot \mathbf{J}_i \quad (i = 1, \ldots, N), \tag{2}$$

where G_i and R_i are the possible generation and absorption rates, respectively. Solving Eqs. (1) and (2) with ion-specific boundary conditions in the system yields the precise ionic concentration as a function of time and subsequently the electrical model.

A. Nonfaradaic interfaces

In the case of IPE, charge cannot pass across the interface, but it can couple to the other conductive phase, which makes the behavior of such interfaces resemble a capacitor [Fig. 1(a)]. For a given potential, there exist a sheet charge on the metal electrode (q^M) and a distributed charge in the solution (q^S). The charge in solution (q^S) is made up of an excess of either cations or anions in the proximity of the electrode surface [Fig. 1(b), double layer[22]]. Gouy[23] and Chapman[24] independently proposed the idea of this diffuse ionic layer in the electrolyte and offered a statistical mechanical approach for its characterization. However, their work was later modified by Stern,[25] who considered that the particles cannot approach a surface any closer than their ionic radius. The general solution for the spatial charge density for a system with multiple ionic species is involved. Nevertheless, the simple solution for the spatial potential from Eqs. (1) and (2) in a system containing only a symmetrical electrolyte (electrolyte having only one cationic spe-

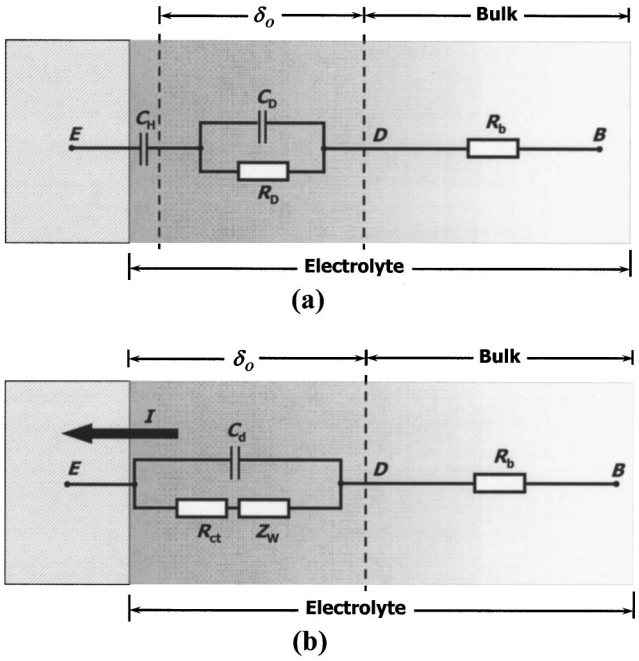

FIG. 2. Half-cell small-signal circuit model of (a) an IPE, and (b) a faradaic electrode.

cies and one anionic, both with charge magnitude z) and total potential difference of Φ_0 on the interface, is expressed by[26]

$$\Phi(x)=\frac{4kT}{zq}\tanh^{-1}\left[\exp(-\kappa x)\tanh\left(\frac{zq}{4kT}\Phi_0\right)\right], \tag{3}$$

where κ, the Debye length, is defined as

$$\kappa=\left(\frac{2n^0z^2q^2}{\epsilon_r\epsilon_0kT}\right)^{1/2}. \tag{4}$$

In Eq. (4), n^0 is the bulk concentration, ϵ_0 is the permittivity of free space, and ϵ_r is the relative permittivity of the solution. The interfacial differential capacitance of the double layer, C_d based on the model just explained is

$$C_d=A\frac{\partial\sigma^M}{\partial\Phi_0}=A\left(\frac{2z^2q^2\epsilon_r\epsilon_0n^0}{kT}\right)^{1/2}\cosh\left(\frac{zq\Phi_0}{2kT}\right), \tag{5}$$

where σ^M is the surface charge concentration on the electrode, and A is the fraction of the electrode surface where $d\Phi/d\hat{\nu}=0$ ($\hat{\nu}$ is unit transverse vector on surface A). Using Stern's approach, we consider a linear potential drop perpendicular to this interface plane to x_1; yet, Eq. (5) still holds for $x\geqslant x_1$. If $\Phi(x_1)=\zeta$ (zeta potential), then the equation for the interfacial differential capacitor can be rewritten as

$$\frac{1}{C_d}=\frac{x_1}{A\epsilon_r\epsilon_0}+\frac{1}{A\cdot\left(\frac{2z^2q^2\epsilon_r\epsilon_0n^0}{kT}\right)^{1/2}\cosh\left(\frac{zq\zeta}{2kT}\right)}, \tag{6}$$

which indicates that the capacitance consists of two components that are exactly as one would find for capacitors in series. Thus, we can identify the terms presented in Eq. (6) as the reciprocal of component capacitances, C_H and C_D, which can be depicted as in Fig. 2(b):

$$\frac{1}{C_d}=\frac{1}{C_H}+\frac{1}{C_D}. \tag{7}$$

C_H is independent of potential and corresponds to the capacitance of the charges held in the inner layer, whereas C_D is the capacitance of the diffused charge. A typical value for C_d is 10–20 μF/cm^2, which is typically dominated by C_D.[1]

To complete the electrical model of the electrode–electrolyte interface, we also need to put the equivalent resistances of the ionic layer and electrolyte into the model. The charges in the inner layer, to a first approximation, are immobile. Consequently, defining a finite resistance for this region is questionable. On the other hand, the ions in the diffusion layer, even though confined by the electric field, are, in fact, mobile. The charged species in this layer can, in fact, move both by drift and diffusion. As a result, an effective distributed resistance R_D can be defined for this layer, which generally differs from the bulk solution resistance R_b [Fig. 2(a)].

The actual value of equivalent circuit components is a function of spatial electric field (i.e., bias conditions of the system), type of ions present in the solution, and the reactivity and affinity with the surface. However, one can assume that for sufficiently small perturbations (e.g., small signals), they behave as ideal passive components. In the case of noise modeling, the inherent low-amplitude nature of the observed processes, allows us to consider all of these components to be noise independent and unchanging, thus avoiding the complications of large signal distortion.

B. Faradaic interfaces

In faradaic electrodes, specific charged species (oxidizing species O and reducing species R) can transfer charge between the electrolyte and the electrode. To derive the ionic concentrations in faradaic electrodes, it is enticing to use Eqs. (3) through (7). However, the system is not in thermal equilibrium, so that the conditions for applicability of Eq. (3) are not met. The alternative approach is to use a simplified model where a stagnant layer of thickness $\delta_0(t)$ near the surface of the electrode (Nernst diffusion layer[1]) is assumed. Assuming that the bulk solution has high electrical conductance, one can consider that all of the electric field, either generated by an external source or intrinsic potential difference of the electrode–electrolyte, exists solely within this layer. It is also critical to understand that the profile of the ions, and $\delta_0(t)$ are functions of the bulk concentration, electric field, and the temporal current passing through the interface.

The Nernst diffusion layer can be expressed as the nonequilibrium state of the double layer, where single or multiple charged species are constantly transferring charge at the interface, creating a net current passing through the electrode. A simple yet useful method is to approximate the layer with a linear concentration profile for ions from bulk to the surface with thickness $\delta_0(t)$ (generally about 1–10 μm), instead of an expected pseudo-exponential form. The net charge concentration in this region has a linear profile, re-

sulting in a quadratic electric field function throughout the layer. With this approximation, the interfacial differential capacitance of the diffusion layer, C_d becomes

$$C_d = A\frac{\partial Q_T}{\partial \Phi_0} = A\frac{3\epsilon\epsilon_0}{\delta_0}. \tag{8}$$

The complete model requires an electrical element parallel to the diffusion capacitance, which represents the faradaic process. This element is usually called the faradaic impedance,[1] which is typically separated into a pure charge transfer resistance R_{ct}, and Z_{W}, the Warburg impedance.[27,28] At low frequencies, the effect of Warburg impedance can be neglected and the element in series with the diffusion impedance is merely R_{ct}, defined as a function of flowing current i as

$$R_{\mathrm{ct}} = \left(\frac{di}{d\Phi_0}\right)^{-1}. \tag{9}$$

The charge transfer resistance with a small overpotential can be derived from the Butler–Volmer relationship[29,30] as a function of total redox current i_T

$$R_{\mathrm{ct}} = \frac{kT}{zq}\left|\frac{1}{i_T}\right|. \tag{10}$$

The circuit model of the faradaic electrode in the presence of oxidation and reduction becomes very similar to the IPE model, except for the faradaic impedance.

While the models presented in Fig. 2 eventually break down as we shrink the physical sizes towards mesoscopic regimes (since the number of particles in the vicinity of the sensor becomes very small and statistical averaging is not justified), they are still valid for a major fraction of the practical size range of interest. Furthermore, the models provide an excellent vehicle with which to predict the general trend in scaling of sensor electrodes, as do the models presented in later sections.

III. NOISE MODELING

The origins of electrical fluctuation in electrode–electrolyte systems can be divided into two categories: thermal equilibrium fluctuations, which is typically the case in IPE systems, and nonequilibrium fluctuations in the systems where recombination and generation of charged particles are present (i.e., faradaic electrodes). Thermal equilibrium fluctuations are the only noise sources under equilibrium conditions. The fluctuation dissipation theorem of thermodynamics[31] states that, in thermal equilibrium, the noise properties of a system can be fully characterized by identifying its dissipative processes. Applying the theorem to the electrode–electrolyte systems, one concludes that for IPE systems in thermal equilibrium, the noise of the system is fully modeled by associating a white current noise source with each individual resistor in the circuit model. The power spectral density of this noise would be $4kT/R$ (R being the resistance) dictated by the Johnson–Nyquist[32,33] formulation of thermal noise. The distributed capacitors remain noise-free since they do not dissipate any energy.

In the vicinity of faradaic electrodes, on the other hand, the system is driven well into nonequilibrium. The total noise

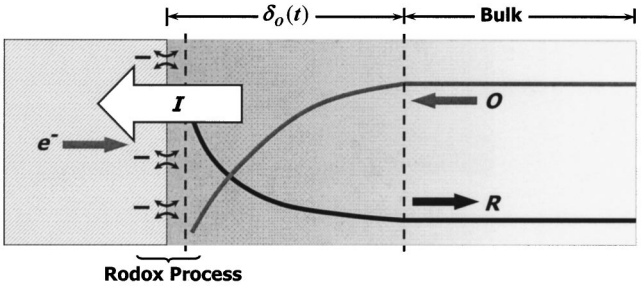

FIG. 3. Pathway of a general electrode redox reaction.

of the system comprises not only the thermal noise sources associated with dissipative elements, but also the nonequilibrium fluctuations due to charge transfer. To quantify the effect of this specific noise source, one should notice that the total observed current in the electrode–electrolyte interface is the sum of all of individual molecular level relocations. Each molecular mass relocation (Fig. 3) can be a combination of drift and diffusion processes at the double layer and interface proximity. By assuming that the transport phenomena of a single process are mutually independent (an appropriate assumption for macroscopic electrodes), each contributing an identical electrical current wave form $i(t)$ to the total current $i_T(t)$, we can calculate the external current spectra by means of Carson's theorem.[31] In the following section, we carry out a comprehensive analysis on the spectral characteristics of current fluctuation in view of various realistic electrical conditions.

A. Single-event current signature characteristics

As an illustrative scenario of nonequilibrium systems, consider a single redox process in which an oxidized species is moved to the surface from the bulk by mass transfer processes (Fig. 3). As a result, the reduced species is released and transported back into bulk. The overall process creates an electrical current where some equivalent electrons are transported into the electrolyte from the solution or vice versa. Depending on the physical characteristics of the electrode–electrolyte interface, the shape of the generated wave form varies. Yet, the traversal course of action (for both oxidized species) has an expected duration. Here, we introduce τ_t, the transit time, as the time where the single event is initiated to the end of its mass transfer. The transit time, in practical applications, can vary between 10 and 1000 μs, depending on the electrode polarization and the precise mass relocation process. The total transferred charge from the bulk to the conductor $[Q(t)]$ in view of the transit time, has the following characteristics

$$\begin{aligned} &Q(t) = 0, \quad \text{if } t \leqslant 0, \\ &Q(t) = zq, \quad \text{if } t \geqslant \tau_t. \end{aligned} \tag{11}$$

The external current $i(t)$ produced by this charge transfer procedure is defined as $i(t) = dQ(t)/dt$, hence

$$\begin{aligned} &i(t) = 0, \quad \text{if } t \leqslant 0 \quad \text{and } t \geqslant \tau_t, \\ &i(t) \neq 0, \quad \text{if } 0 \leqslant t \leqslant \tau_t, \end{aligned} \tag{12}$$

$$\int_0^\infty i(\alpha)d\alpha = zq. \tag{13}$$

While $i(t)$ bears the necessary information to characterize to electrode system as well as redox kinetics, the observed external current $i_O(t)$ does not. There are two extreme regimes for observed current: (i) The external circuit relaxation time τ_C is much larger than the transit time of the process ($\tau_C \gg \tau_t$), and (ii) when the system response time is much faster than the charge transfer and mass relocation kinetics ($\tau_C \ll \tau_t$). In the first case, the response of external circuitry specifies the observed current fluctuation spectra, contrary to the latter, in which the current spectra contain the unperturbed kinetics of the individual charge transfer processes. Each of these regimes is now considered.

B. Noise current power spectral density when ($\tau_C \gg \tau_t$)

In this scenario, the charge transfer due to the redox processes, occurs almost instantly, whereas the relaxation time constant τ_C through the external circuit is much slower. In terms of impedances, this implies that the mass transfer required time, represented by the Warburg impedance, is negligible compared to the delay through the external circuitry. Thus, $i_O(t)$ becomes

$$i_O(t) = \frac{zq}{\tau_C}\exp\left(-\frac{t}{\tau_C}\right). \tag{14}$$

Accordingly, the power spectral density of total current $i_O(t)$ defined by $S_i(\omega)$, can be derived, again using Carson's theorem[31]

$$S_i(\omega) = 2\nu|I_O(j\omega)|^2 + 4\pi\nu^2\left|\int_{-\infty}^{+\infty} i_O(\tau)d\tau\right|^2 \cdot \delta(\omega)$$

$$= 2\nu(zq)^2\left(\frac{1}{1+\tau_C^2\omega^2}\right) + 4\pi\nu^2(zq)^2\cdot\delta(\omega), \tag{15}$$

where $I_O(j\omega)$ is the Fourier transform of $i_O(t)$ and ν is the average event rate. The dc component of current is specified by the average rate of charge transferred defined by $i_T = zq\nu$, consequently, Eq. (15) can be rewritten as

$$S_i(\omega) = \frac{2zqi_T}{1+\tau_C^2\omega^2} + i_T^2[4\pi\delta(\omega)]. \tag{16}$$

By removing the dc value from Eq. (16), the current noise power spectral density $S_i^N(\omega)$ in the low-frequency region, where $\omega \ll 1/\tau_C$, becomes

$$S_i^N\left(\omega \ll \frac{1}{\tau_C}\right) = 2zqi_T, \tag{17}$$

which is shot noise in its general form. This result was expected conceptually, since a potential barrier exists for the charged species at the interface. This type of shot noise behavior was previously reported independently.[12–15] It is also imperative to observe that while the noise spectrum is proportional to the current flowing through the system, the charge of the ions participating in the reaction also affects the fluctuation magnitude.

C. Noise current power spectral density when ($\tau_C \ll \tau_t$)

1. General low-frequency region

When the system response time is fast enough that it does not affect the original impulse current of the redox process (e.g., short-circuit current), the aggregate current generated is the superposition of all individual charge relocation events defined in Eq. (12), without significant distortion [i.e., $i_O(t) = i(t)$]. Based on Eq. (15), the spectral density of the short-circuit current in a half-cell electrode system such as the one in Fig. 2 is

$$S_i(\omega) = 2\nu\left[\frac{R_{\rm ct}}{R_{\rm ct}+R_b}\right]^2|I_O(j\omega)|^2$$

$$+ 4\pi\nu^2\left[\frac{R_{\rm ct}}{R_{\rm ct}+R_b}\right]^2\left[\int_{-\infty}^{\infty} i_O(\tau)d\tau\right]^2\delta(\omega). \tag{18}$$

By substituting Eq. (13) in Eq. (18) and defining the constant $\beta = R_{\rm ct}/(R_{\rm ct}+R_b)$, we can rewrite Eq. (18) as

$$S_i(\omega) = \left(\frac{2i_T\beta^2}{zq}\right)|I_O(j\omega)|^2 + i_T^2\beta^2[4\pi\delta(\omega)]. \tag{19}$$

The second term on the right-hand side of Eq. (19) is once more the observed dc component, and the first term is the noise fluctuation spectral density. If we are to examine the low-frequency region of current noise spectrum, excluding the noise of the bulk resistance for now, the following approximation is valid:

$$S_i^N\left(\omega \ll \frac{1}{\tau_T}\right) \approx \left(\frac{2i_T\beta^2}{zq}\right)|I_O(0)|^2, \tag{20}$$

and by substituting Eq. (13),

$$S_i^N\left(\omega \ll \frac{1}{\tau_T}\right) \approx \left(\frac{2i_T\beta^2}{zq}\right)\left|\int_{-\infty}^{\infty} i_O(\alpha)d\alpha\right|^2, \tag{21}$$

hence

$$S_i^N\left(\omega \ll \frac{1}{\tau_T}\right) \approx 2zqi_T\beta^2. \tag{22}$$

In this scenario, if the electrolyte is highly conductive, β reaches unity, indicating once more the general form of shot noise presented in Eq. (17). This answer is in fact consistent with the noise spectra calculated in the previous subsection, since at relatively low frequencies, both Warburg and diffusion capacitance plus the impedances representing external relaxation time become negligible, ensuing the same noise spectrum.

2. Mass-transfer processes effects on high frequency noise spectral density

In the previous subsection, we looked at the low-frequency region of the noise spectrum in electrode systems. If we examine Eq. (19), and isolate the current fluctuation,

TABLE I. The calculated noise spectrum of various mass transfer processes. m and μ are the effective mass and mobility of the charged species, respectively. The high-frequency envelope of the noise spectrum is also predicted in the right column, which suggests a major difference between spectral density of drift and diffusion dominant processes.

Mass transfer	$\nu(t)$	τ_t	$S_i^N(\omega)/2zqi_T$	$S_i^N(\omega \gg \tau_t^{-1})$
Drift constant velocity	$\nu_0=\mu E$	$\frac{\delta_0}{\mu E}$	$\left[\mathrm{sinc}\left(\frac{\tau_t\cdot\omega}{2}\right)\right]^2$	$\propto\frac{1}{\omega^2}$
Drift constant acceleration	$a_0 t=\left(\frac{qE}{m}\right)\cdot t$	$\sqrt{\frac{2m\delta_0}{qE}}$	$\frac{4\cdot\lvert j+(\tau_t\omega-j)\cdot e^{-j\tau_t\omega}\rvert^2}{\tau_t^2\cdot\omega^4}$	$\propto\frac{1}{\omega^2}$
Diffusion	$\sqrt{\frac{2D}{t}}$	$\frac{\delta_0^2}{8D}$	$\frac{\pi\cdot\lvert\mathrm{erf}(\sqrt{j\tau_t\omega})\rvert^2}{4\sqrt{\tau_t\omega}}$	$\propto\frac{1}{\omega}$

we notice that the precise high-frequency noise spectral density relies solely on individual current signature in view of mass transfer processes present at the interface. If we disregard the mass relocation due to convection (i.e., no stirring), the charge transfer process and the movement of the electroactive species can be predicted by calculating the effects of drift and diffusion.

By means of the Shockley–Ramo theorem,[34,35] one can formulate the relationship between the current and the charged species velocity $\nu(t)$ during the transit time. Using this theorem, in the stagnant layer of thickness δ_0, the overall current from an individual relocation can be expressed by

$$i(t)=\frac{zq\nu(t)}{\delta_0}[u(t)-u(t-\tau_t)], \tag{23}$$

with a Fourier transform of

$$I(j\omega)=\frac{2zq}{\delta_0}\mathcal{F}\{\nu(t)\cdot u(t)\}*\left[\frac{\sin(\omega\cdot\tau_t)}{\omega}\right], \tag{24}$$

which one can subsequently place into Eq. (19) to evaluate the noise spectrum. To better grasp the high-frequency behavior of the noise, we can examine distinctive regimes of mass transfer (Table I). In an electrode system in which drift is the dominant mass transfer process (e.g., highly polarized interface), an electro-active species with unchanging relocation velocity [$\nu(t)=\nu_0$, for $0\leqslant t\leqslant\tau_t$] can generate the following current

$$i(t)=\frac{zq\nu_0}{\delta_0}[u(t)-u(t-\tau_t)]=\frac{zq}{\tau_t}[u(t)-u(t-\tau_t)]. \tag{25}$$

The power spectral density of such a process based on Eq. (19) becomes

$$S_i^N(\omega)=2zqi_T\left[\mathrm{sinc}\left(\frac{\tau_t\omega}{2}\right)\right]^2. \tag{26}$$

Using a similar approach, we can calculate and subsequently plot the expected noise power spectral density of drift dominant processes with accelerating velocity, as well as diffusion dominant electrodes (see Table I and Fig. 4). It is imperative to realize that the diffusion velocity,[1,36] defined at diffusion-dominant interfaces, has a $t^{-1/2}$ time dependency, since random walks (the fundamental process responsible for diffusion) greatly favor small displacements from the starting point (i.e., electrode interface). This unique velocity wave form, not present in drift processes, is the key factor creating $1/f$ behavior in the noise spectrum, as will be discussed shortly.

Plotting the calculated current noise spectral densities of Table I, and comparing their overall shape to the reported data,[18,19] reveals numerous spectral similarities. The first observation is that, as predicted in subsection 1, the low-frequency spectrum of all current noise, independent of the interface, reaches a plateau in the low-frequency region, with a height proportional to the passing current amplitude. However, there are significant dissimilarities in the high-frequency noise spectrum of surfaces, depending on the specific mass transfer processes present at the interface.

In highly polarized faradaic interfaces (e.g., copper or mild steel in sea water) a low-frequency plateau with a $1/f^2$ roll off has been reported.[19] This reported spectral profile can be explained using our models for drift-dominant processes [Figs. 4(a) and 4(b)]. As seen in Fig. 4, the model points out that $1/f^4$ is an indication of constant acceleration for the ionic species, and $1/f^2$ at high frequency suggests drift-dominant relocation processes in general. Furthermore, diffusion-dominant electrodes, in contrast to drift-dominant systems, can explain $1/f$ noise spectrum, which is similar to the reported $1/f$ spectra at corrosive interfaces. It can be argued that an electrode system with corrosion (i.e., slow redox processes) is basically nonpolarized (i.e., low interfacial electric field) which leads to only diffusion movements with little drift. This results in a $t^{-1/2}$ time dependency for velocity, which in turn implies a $1/f$ spectrum.

Based on our model, in all three cases, a sharp peak in the spectrum is expected adjacent to the plateau region. This phenomenon has also been observed and reported in the literature in the case of crevice attack.[19] Based on the mathematical models discussed here, we can postulate that it originates from large values of τ_t possibly present in this type of interface, which shift the peak toward lower frequency regions, away from the thermal noise floor. The same rationale can be used again to explain any discrepancy in the literature when the peak is not observable and probably buried in the thermal noise originating from the resistors.

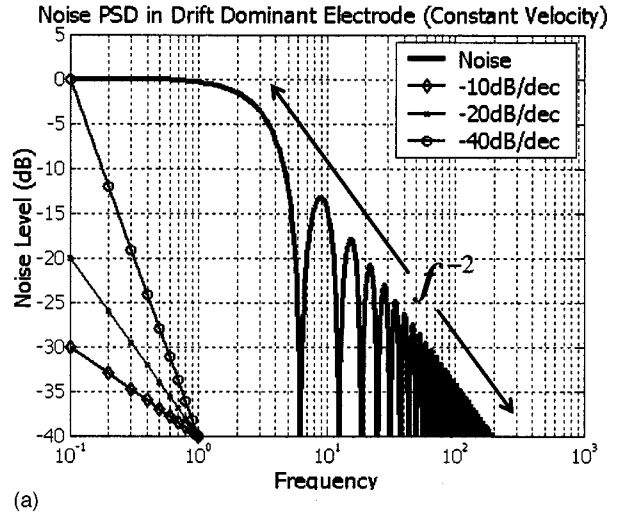

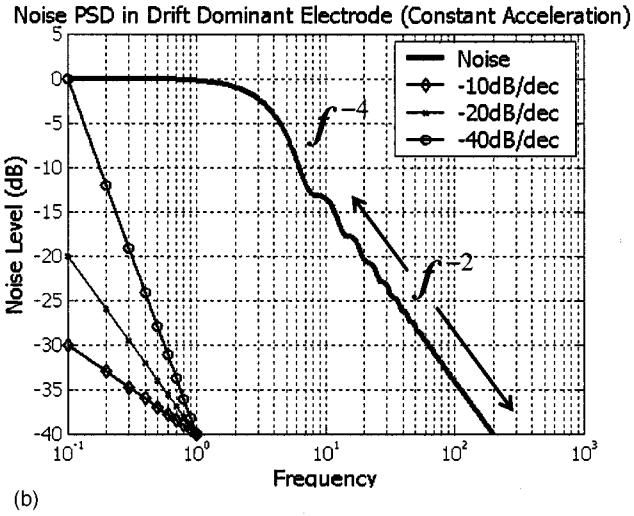

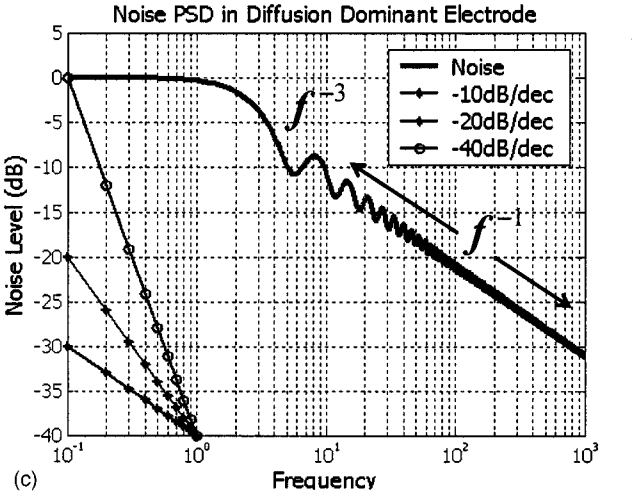

FIG. 4. Normalized noise power spectral density of electrode systems with (a) drift dominant mass transfer process and constant velocity, (b) drift dominant mass transfer process and constant acceleration, and (c) diffusion dominant mass transfer process.

D. Noise circuit model

As mentioned in the previous sections, spontaneous current or voltage fluctuations in typical electrode–electrolyte systems originate from energy dissipative conductors and

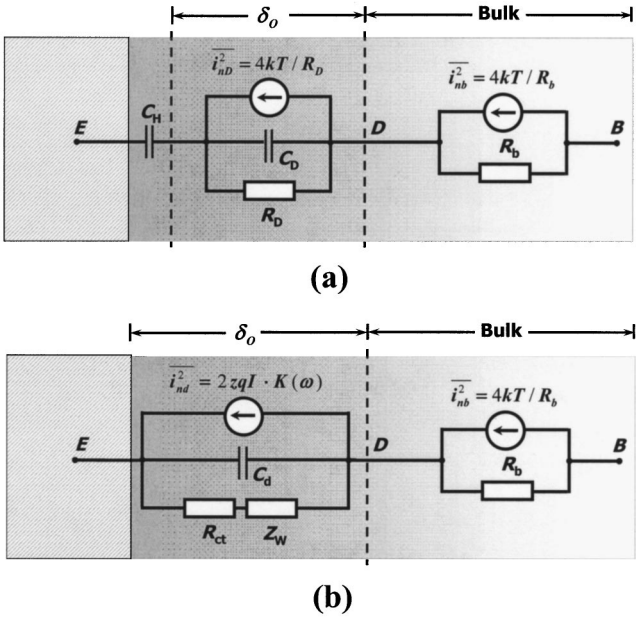

FIG. 5. Noise circuit model of an (a) IPE and faradaic electrode (b).

electrochemical interactions. In Fig. 5(a), we present the half-cell noise circuit model of a nonfaradaic electrode in equilibrium, where the diffusion layer resistance and the bulk resistance are the only energy dissipating terms and therefore the main sources of noise. A circuit model for an electrode with a faradaic process is also presented in Fig. 5(b), where nonequilibrium noise as well as thermal noise is present. The observed fluctuation in this particular system results from two independent noise sources, with dissimilar inherent noise processes. The function $K(\omega)$ represents the specific mass transfer effect at the interface, modifying the full shot noise model. The exact function can be can be extracted from Table I.

For the case of small-scale sensors or electrode systems in general, the present models are still valid as long as statistical averaging is justified. In the case of a macroscpic IPE sensor in equilibrium, we are looking at the uncertainty of the voltage on the interface capacitor. It can easily be shown that the fluctuation of the voltage on this capacitor is inversely proportional to the capacitance (the variance of the capacitor voltage is kT/C at any given time). This implies that by scaling down the electrode, the uncertainty of the voltage appearing on the sensor increases. On the other hand, in the case of faradaic electrodes, we are relying on the current measurement to carry out the sensing. Consequently, a good measure for sensor accuracy will be $(\Delta i_T/i_T)^2$. In the presence of shot noise, this value becomes inversely proportional to i_T. Hence, by maintaining a constant current density, the relative uncertainty of the current becomes inversely proportional to the square of the interface area. It can be seen that in both scenarios, the noise of the sensor greatly increases as the interface size is shrunk. In view of this, as we scale down individual electrochemical systems to micro- and nanoscale dimensions, interface noise turns into the main source of uncertainty, overshadowing all other noise sources.

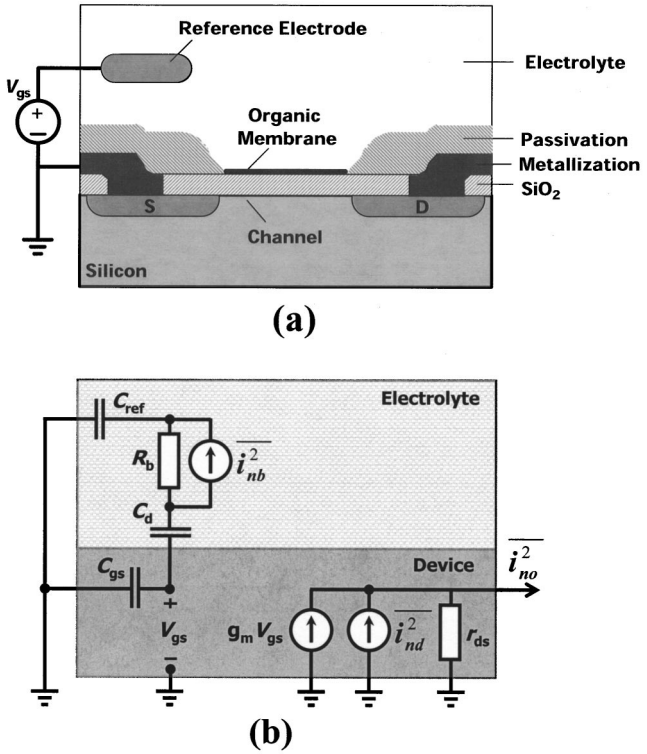

FIG. 6. Ion-sensitive device (a) and its compact circuit model operated in the saturation region (b).

IV. PRACTICAL IMPLICATIONS

A. Battery noise

Batteries typically have two faradaic electrodes that share the electrolyte. In most practical applications in electronics, the batteries not only have a huge internal capacitance (due to the large electrode area and high ionic strength of the electrolyte), but also are often placed in parallel with additional external capacitances. While for such arrangements almost all high-frequency noise is suppressed, there still exists a low-frequency component of shot noise due to the inherent faradaic processes. If we assume that the two electrodes engage in z_1 and z_2 electron transfer processes, respectively, the total low-frequency current noise spectrum $\overline{i_{\mathrm{no}}^2}(\omega)$, based on Eq. (22), becomes

$$\overline{i_{\mathrm{no}}^2}(\omega)=2qi_T\left[\frac{z_1\cdot R_{c1}+z_2\cdot R_{c2}}{R_{c1}+R_{c2}+R_b+R_{\mathrm{load}}}\right], \tag{27}$$

where R_{c1} and R_{c2} are the charge transfer resistances of the electrodes defined by Eq. (10), R_b is once more the bulk resistance, and R_{load} is the load impedance.

B. Ion-sensitive field effect transistor noise

ISFETs are a family of steady-state electrochemical sensors[9,10] which basically employ the structure of a metal-oxide-semiconductor FET without the gate contact. In ISFETs, the gate insulator is directly exposed to the ionic medium under experiment. In this structure, the drain current (flowing between the gate and the source), can be effected through the confined charge in the double layer [Fig. 6(a)]. An external faradaic reference electrode is typically required in the system for stabilization, although the gate acts as a nonfaradaic electrode and no net current theoretically flows through during sensing. As shown in Fig. 6(b), the main noise sources of this particular system operated in the saturation region, are the electrolyte thermal noise (both in the bulk and the diffusion layer), and the drain current noise.

The output current noise spectral density of the system $\overline{i_{\mathrm{no}}^2}(\omega)$, with internal FET drain current noise of $\overline{i_{\mathrm{nd}}^2}(\omega)$, is

$$\overline{i_{\mathrm{no}}^2}(\omega)=\overline{i_{\mathrm{nd}}^2}(\omega)+4kTR_b\left[\frac{C_{\mathrm{gs}}}{C_{\mathrm{gs}}+C_{\mathrm{ref}}+C_d}\right]^2\left[\frac{\omega^2}{\omega^2R_b^2+1}\right], \tag{28}$$

where C_{gs} is the gate capacitance, C_d the double-layer capacitance, and C_{ref} the diffusion layer capacitance of nonfaradaic reference electrode.

V. CONCLUSION

The observed current noise spectral density from electrochemical systems, comprising of electronic conductors (electrodes) and ionic conductors (electrolytes), originates from two main sources. Typically, when there is no net current flowing through the interface, which corresponds to no charge transfer process present at the interface (i.e., nonfaradaic electrodes), only thermal noise is anticipated. Hence, the spectral density of the measured noise relies on the macroscopic equivalent circuit model of the setup, and its possible frequency dependencies. Conversely, in the case in which charge transfer occurs at the interface, a current-dependent fluctuation becomes apparent (i.e., shot noise), in addition to incessant thermal noise, originating from all dissipative components. The excess shot noise is inherently frequency dependent, and its exact spectrum is denoted by the charge transfer and mass transfer processes of the electro-active species, in proximity of the interface. If the mass transfer process is dominated by electric field effects, the noise spectra possess a $1/f^2$ dependency, while in diffusion-dominant electrodes, ionic relocation can potentially bring about excess noise obeying an inverse frequency power law (i.e., $1/f$ noise).

Fundamental noise circuit models have been presented in this article and the general method for their derivation potentially can be implemented to analyze and predict the noise behavior of various electrochemical systems and their correlation with scaling for future micro- and nanodevice applications.

ACKNOWLEDGMENT

This research was supported by NSF in support of the Network for Computational Nanotechnology (NCN).

[1] A. J. Bard and L. J. Faulkner, *Electrochemical Methods: Fundamentals and Applications*, 2nd ed. (Wiley, New York, 2001).
[2] G. T. A. Kovacs, *Micromachined Transducers Sourcebook*, 1st ed. (McGraw Hill, New York, 1998), Chap. 8, p. 688.
[3] P. Bergveld, IEEE Trans. Biomed. Eng. **17**, 70 (1970).
[4] P. Bergveld, Sens. Actuators B **4**, 125 (1991).

[5] D. H. J. Baert and A. A. K. Vervaet, J. Power Sources **114**, 357 (2003).
[6] D. Linden, *Handbook of Batteries*, 3rd ed. (McGraw Hill, New York, 2001).
[7] R. Thewes *et al.*, Proc. Int. Solid-state Circuits Conf. (ISSCC), San Francisco, 2002, p. 350.
[8] Y. Cui, Q. Wei, H. Park, and C. Lieber, Science **293**, 1290 (2001).
[9] J. Fritz, E. Cooper, S. Gaudet, P. K. Sorger, and S. Manalis, Proc. Natl. Acad. Sci. U.S.A. **99**, 14142 (2002).
[10] R. Hintsche, M. Paeschke, U. Wollenberger, U. Schnakenberg, B. Wagner, and T. Lisec, Front. Biosensorics **80**, 267 (1997).
[11] J. Wang, Anal. Biochem. **71**, 328R (1999).
[12] V. A. Tyagai, Electrochim. Acta **16**, 1647 (1968).
[13] K. J. Euler, Elektrotech. Z., ETZ **24**, 115 (1974).
[14] G. Blanc, C. Gabrielli, and M. Keddam, Electrochim. Acta **20**, 687 (1975).
[15] G. Blanc, I. Epelboin, C. Gabrielli, and M. Keddam, J. Electroanal. Chem. **75**, 97 (1977).
[16] I. Epelboin, C. Gabrielli, M. Keddam, and L. Raillon, J. Electroanal. Chem. **105**, 389 (1979).
[17] W. P. Iverson, J. Electrochem. Soc. **115**, 617 (1968).
[18] K. Hladky and J. L. Dawson, Corros. Sci. **21**, 317 (1981).
[19] K. Hladky and J. L. Dawson, Corros. Sci. **22**, 231 (1982).
[20] C. Gabrielli, F. Huet, and M. Keddam, J. Chem. Phys. **99**, 7232 (1993).
[21] E. Huigen, A. Peper, and C. A. Grimbergen, Med. Biol. Eng. Comput. **40**, 332 (2002).
[22] B. E. Conway, *Theory and Principles of Electrode Processes* (Ronald, New York, 1965), Chaps. 4, 5.
[23] G. Gouy, Compt. Rend. **149**, 654 (1910).
[24] D. L. Chapman, Philos. Mag. **25**, 475 (1913).
[25] O. Stern, Z. Elektrochem. **30**, 508 (1924).
[26] D. C. Grahame, Annu. Rev. Phys. Chem. **6**, 337 (1955).
[27] J. R. McDonald, *Impedance Spectroscopy: Emphasizing Solid Materials and Systems*, 1st ed. (Wiley, New York, 1987).
[28] J. Gunning, D. Y. C. Chan, and L. R. White, J. Colloid Interface Sci. **170**, 522 (1995).
[29] J. A. V. Butler, Trans. Faraday Soc. **19**, 729 (1924).
[30] T. Erdey-Gruz and M. Volmer, Physik. Chem. **15A**, 203 (1930).
[31] A. Van der Ziel, *Noise in Solid State Devices and Circuits*, 9th ed. (Eilry, New York, 1986).
[32] J. Johnson, Phys. Rev. **32**, 97 (1928).
[33] H. Nyquist, Phys. Rev. **32**, 110 (1928).
[34] W. Shockley, J. Appl. Phys. **9**, 635 (1938).
[35] S. Ramo, Proc. IRE **27**, 584 (1939).
[36] I. Karatzas and S. E. Shreve, *Brownian Motion and Stochastic Calculus*, 2nd ed. (Springer-Verlag, New York, 1991), Vol. 1, Chap. 2, p. 47.